Stopping cross section of bulk graphite for α particles*

S. Matteson, E. K. L. Chau, and D. Powers
Baylor University, Waco, Texas 76703
(Received 23 February 1976)

The stopping cross section of bulk graphitic carbon for α particles of energy 0.3–2.0 MeV has been measured absolutely and relative to vapor-deposited carbon, and is found to be $\sim$ 6–28% higher than the corresponding value of vapor-deposited carbon. The difference is attributed to an allotropic effect.

I. INTRODUCTION

Extensive stopping cross-section measurements of hydrocarbons made by us and our co-workers have suggested that the stopping cross section of carbon in a molecule, as determined by Bragg-rule-type calculations, is dependent upon the nature and strength of the carbon bonds.[1-5] These carbon stopping-cross-section values are compared to the elemental, or atomic, stopping cross section obtained from amorphous vapor-deposited thin carbon films.[6-9] However, electron diffraction studies reveal that rather than consisting of isolated, unbonded carbon atoms, amorphous thin carbon films may be constituted of microscopic ($\lesssim$10 Å) regions of ordered, covalently bonded carbon.[10] Moreover, some researchers have observed in vapor-deposited carbon C-C bond lengths typical of *both* diamondlike single bonds as well as graphitelike delocalized double bonds.[11] Furthermore, Softky[12] found that the relative stopping cross section of diamond for protons is 6% less than that of graphite for protons of 1.1-MeV incident energy. Northcliffe and Schilling,[13] on the other hand, reported a significantly lower proton stopping cross section for vapor-deposited carbon at 1.1 MeV than Softky. These considerations recommend that a careful measurement be made of the stopping cross section of graphite for α particles.

Previous measurements of the stopping cross section of carbon were performed using a thin-target method, which required a vapor-deposited film of known areal density.[6-9] In order to form such a film, carbon was evaporated by heating it to over 1800 °C[9,14,15] in a carbon arc at high vacuum. The evaporation generates the highly reactive components of carbon vapor, C_1, C_2, C_3,[16] which can bond covalently with other carbon atoms upon striking the growing film, forming various ring structures. Thus, the film is, at best, of uncertain allotropic form.

The present experiment differs from a thin-film experiment in that (i) use is made of a thick target of bulk graphite, whose allotropic form is well known[17] to be a six-membered benzenelike structure with delocalized double bonds, and (ii) the thick-target method of Wenzel and Whaling[18] is employed. The purpose of the present experiment is to measure the stopping cross section of the carbon allotrope, graphite, absolutely and relative to vapor-deposited thin-film carbon, and to determine if any allotropic, or valence, effect is observable in the elemental stopping cross section.

II. TARGET PREPARATION

Graphite targets were prepared from 99.98% pure polycrystalline graphite from Union Poco Graphite, Inc., Decatur, Tex. The blanks were first sanded with dry emery polishing paper, then buffed with dry tissue, then with micropolishing cloth charged either with 0.05-μ alumina or with powdered graphite, and buffed again with tissue. The scattering spectra (see Sec. III) from these targets were always carefully examined for evidence of contamination, either by the polishing agents or by organic contaminants from the vacuum pumps, but no contamination was observed.

A careful microscopic study of the surface morphology of the graphite samples revealed that the fractional area covered by any pores or scratches was less than 0.1%. Excessive roughness could cause significant error,[19] but no observable variation in scattering yield was observed from targets having average pore size from $\simeq$10 μm to the typical size of $\simeq$0.4 μm. X-ray diffraction patterns from scrappings of the graphite samples revealed sharp rings with d spacings in agreement with accepted standards for graphite.[20] The crystallite size specified by the manufacturer was <0.001 in., and since the beam spot averaged over $\sim 10^5$ randomly oriented crystallites, channeling effects are believed to be negligible.

As a check of the experimental method and as a means of determining if an allotropic effect exists in graphite and vapor-deposited carbon, 50–100 μg/cm^2 thick targets of evaporated carbon were also prepared and analyzed by the method given in

Sec. III. Both spectrographic-grade rods and rods formed from the Poco graphite samples were used in a carbon arc and evaporated onto a highly polished Be substrate or onto a thin layer of Ag or Au on top of the polished graphite. This procedure was followed so as to eliminate any possibility that different surface finishes of the Be or graphite would give different scattering yields; no observable difference was seen.

Electron and x-ray diffraction patterns of the vapor-deposited C films showed very diffuse rings typical of amorphous[21] C. It is therefore concluded that the graphite and the amorphous vapor-deposited targets used in the experiment were indeed two distinct forms of C.

Heating of the target due to the incident He ion beam was also considered, since it could alter the identity of the target. Calculations of the maximum temperature rise of the irradiated target indicated that the carbon-film temperature never exceeded and was typically much less than 100 °C, which is well below the minimum annealing temperature[22] (400 °C) required to affect substantially the structure of the thin carbon film.

III. EXPERIMENTAL PROCEDURE

The detailed experimental arrangement for stopping-cross-section measurement by elastic scattering from thick targets is essentially that reported in a previous paper.[23] Briefly, a He^+ ion beam obtained from a 2-MeV Van de Graaff accelerator is focused by a quadrupole magnet, analyzed by a 10° magnet, trimmed to a 1×1-mm spot, and directed into an 18-in. scattering chamber with typical beam current 100 nA. The elastically scattered He^+ ions are detected by a 100-μm silicon surface-barrier detector, and analyzed in a 256-channel multichannel analyzer, where dead-time corrections can be made. The incident beam current is measured by an Elcor current integrator connected to the movable target rod. An electron trap is used which consists of a pair of parallel horizontal plates, one above the beam at ground potential and the other below the beam at −225 V dc. The same negative potential is applied to a thermally and electrically insulated copper baffle surrounding the target. The baffle is in thermal contact with a liquid-nitrogen reservoir, thus providing both secondary electron suppression and cryogenic pumping of residual vapors. This feature is of utmost importance since any extraneous carbon deposited by the cracking of hydrocarbon, e.g., diffusion pump oil, would degrade the detected spectrum. The vacuum was maintained below 2×10^{-6} Torr, a level at which carbon buildup is minimal. The target rod is maintained at a +225 V dc potential in order to inhibit the emission of secondary electrons.

As is shown in Ref. 23, the yield per energy channel is given by

$$y(E_{10},E_{20}) = N_0\Delta\Omega\frac{d\sigma}{d\Omega}\frac{dE_{20}}{\epsilon_{\rm eff}(E_S,E_{20})}, \tag{1}$$

where

$$\epsilon_{\rm eff}(E_S,E_{20}) = \frac{\epsilon(E_{20})}{\epsilon(\alpha E_S)}[\alpha\epsilon(E_S)+\beta\epsilon(\alpha E_S)], \tag{2}$$

with α as the kinematic constant, $\epsilon = dE/N\,dS$ is the stopping cross section, $\beta = \cos\theta_1/\cos\theta_2$, E_S the incident energy at depth S beneath the surface, E_{10} and E_{20} the energy of incident and detected ions at angles θ_1 and θ_2 with the target normal, respectively, and dE_{20} the width of the energy channel. The scattering configuration is shown in Fig. 1, where $\theta_1=\theta_2=45.0°$ and $\theta_L=90.0°$. At the target surface, i.e., at $S=0$, the effective stopping cross section takes the simple form

$$\epsilon_{\rm eff}(E_{10},\alpha E_{10}) \equiv \epsilon_{\rm eff}(E_{10}) = \alpha\epsilon(E_{10})+\beta\epsilon(\alpha E_{10}), \tag{3}$$

which is equivalent to the expression first given by Snyder *et al.*[24]

The number of incident ions N_0 is given by N_0

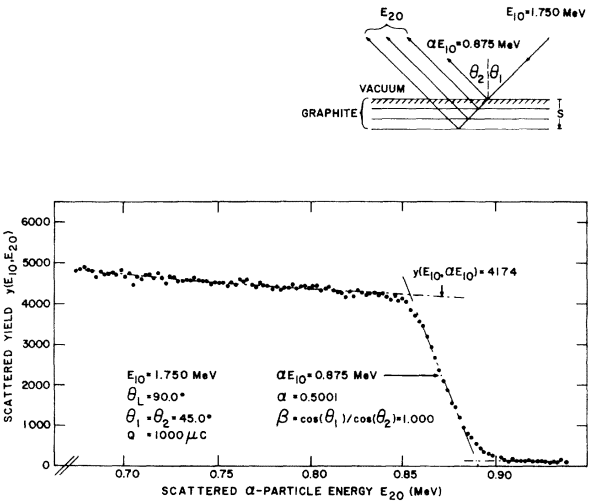

FIG. 1. Elastic scattering of α particles from a thick graphite target at bombarding energy $E_{10}=1.750$ MeV, laboratory scattering angle $\theta_L=90.0°$, and target angles $\theta_1=\theta_2=45.0°$. The scattering yield $y(E_{10},E_{20})$ [Eq. (1)] for scattering energy $E_{20}<0.845$ MeV was fitted to $y=A/E_{20}+B$ and extrapolated to $y(E_{10},\alpha E_{10})=4174$ counts at energy $\alpha E_{10}=0.875$ MeV, which is the energy of the α particles scattered from the graphite surface. The kinematic constant α is $(M_2-M_\alpha)/(M_2+M_\alpha)=0.5001$ at $\theta_L=90.0°$. The effective stopping cross section $\epsilon(E_{10},\alpha E_{10})$ for graphite was calculated from Eqs. (1) and (3) using 41 different spectra of this type.

$= Q/e$, where Q is the total charge collected by the current integrator, and e is the charge per ion. The integrator calibration was frequently checked and found to deviate by no more than a fraction of a per cent for a given target and by no more than 2% during the entire experiment. The scattering yield from a thick polished Ag blank of high purity was measured simultaneously with the carbon scattering yield and under identical experimental conditions in order to check the quantity $N_0\Delta\Omega$ in Eq. (1). The measured Ag yield was compared to that predicted from the Ag stopping cross section of Ref. 23. The mean ratio of measured to predicted scattering yield from the Ag differed from unity by no more than 3%. The integrated charge Q was taken as $N_0 e$, and a probable error of ±3% was assigned to the product $N_0\Delta\Omega$ in keeping with the spread of predicted to measured Ag scattering yields.

The scattering cross section $d\sigma/d\Omega$ used for carbon in Eq. (1) was that of the shell-shielded Coulomb potential of Smith *et al.*[25] The screening of carbon for He^+ ions was calculated to be negligible except for very low energies. The energy per channel was determined by a careful energy-voltage calibration of the detector-preamplifier combination and a voltage-per-channel calibration of the analyzing electronics, the details of which are found in Ref. 23.

The scattering yield at the midpoint of the graphite yield step was determined by curve-fitting the data points over a region extending from $E_{20} \gtrsim \alpha E_{10} - 200$ keV to $E_{20} \lesssim \alpha E_{10} - 30$ keV, where αE_{10} is the energy after scattering from the graphite surface, and extrapolating this curve to the midpoint of the step as illustrated in Fig. 1. Several functional forms were used, e.g., $y = AE_{20} + B$, to fit the data points and gave only minor change in fit. However, the fitting function $y = A/E_{20} + B$ was selected because it gave a very good fit with convenient functional form, and is the one employed in Fig. 1.

This scattering yield y at the midpoint of the step was then used in Eqs. (1) and (3) to find $\epsilon_{\text{eff}}(E_{10})$. Forty-one values of $\epsilon_{\text{eff}}(E_{10})$ from eight different graphite targets were obtained for E_{10} between 0.4 and 2.0 MeV. These $\epsilon_{\text{eff}}(E_{10})$ values were subjected to two independent data-reduction schemes to obtain the actual stopping cross section $\epsilon(E)$, and negligible difference (< 0.25%) was found between the ϵ values from the two schemes. The first scheme was to expand in a Taylor series the functions $\epsilon(E_{10})$ and $\epsilon(\alpha E_{10})$ from Eq. (3) about an intermediate energy E_{int} to obtain

$$\epsilon(E_{\text{int}}) = \frac{1}{\alpha+\beta}\left(\epsilon_{\text{eff}}(E_{10}) - \sum_{n=1}^{\infty}\frac{1}{n!}\left[\alpha(E_{10}-E_{\text{int}})^n + \beta(\alpha E_{10}-E_{\text{int}})^n\right]\frac{d^n\epsilon(E_{\text{int}})}{dE^n}\right), \tag{4}$$

where $\alpha E_{10} < E_{\text{int}} < E_{10}$. $\epsilon(E_{\text{int}})$ is obtained by iteration, first by neglecting the correction terms involving derivatives to obtain an approximate $\epsilon(E_{\text{int}})$, then curve-fitting these 41 values of $\epsilon(E_{\text{int}})$ and taking derivatives to obtain a better $\epsilon(E_{\text{int}})$. The procedure was iterated until the values of $\epsilon(E_{\text{int}})$ did not change with further repetition of the procedure. E_{int} was taken to be $\frac{1}{2}(E_{10} + \alpha E_{10})$ for reliable convergence of the Taylor series, and $\epsilon(E_{\text{int}})$ is thereby limited to $0.3 \leq E_{\text{int}} \leq 1.575$ MeV.

The second data-reduction scheme, which allows a wider energy region $0.2 \leq E \leq 2.1$ MeV but at the expense of slightly increasing the error for $E > 1.5$ MeV, is obtained by approximating the functions $\epsilon(E_{10})$ and $\epsilon(\alpha E_{10})$ from Eq. (3) by a function $F_{a_n}(E)$ to give

$$\epsilon_{\text{eff}}(E_{10}) = \alpha F_{a_n}(E_{10}) + \beta F_{a_n}(\alpha E_{10}), \tag{5}$$

where a_n are the parameters of the fitting function $F_{a_n}(E)$ and are determined by standard least-squares fitting procedures[26] so as to give the best fit to the experimental data points $\epsilon_{\text{eff}}(E_{10})$. The functional form employed in this scheme was the Brice[27] form:

$$\epsilon(x) = F_{a_n}(x) = \frac{4\hbar^2}{5m}\frac{Z_\alpha + Z}{1+(av/v_0)^n}x^{1/2}\frac{30x^2+53x+21}{3(x+1)^2} + (10x+1)\tan^{-1}x^{1/2}, \tag{6}$$

where $a_n = (n, a, z)$, $x = (v/2v_0 z)^2$, $v_0 = e^2/\hbar$, and the α-particle velocity and electron mass are v and m, respectively. Since the scheme may be dependent on the type of function used, five other functions were also tested to determine how much $\epsilon(E)$ would differ from the Brice value. These separate functions were (i) the Bethe-Bloch form with inner-shell corrections suggested by Walske,[28] $F_{a_n}(E) = (a_1/E)\ln(a_2 E) + a_3/E^2 + a_4/E^3$; (ii) a fourth-degree polynomial in E; (iii) $\sqrt{E}$ times type (ii); and (iv) and (v) a smooth joining of $(a_1/E)\ln(a_2 E)$ to types (ii) and (iii), respectively. Type (i) agrees with the Brice form to better than 1% for $0.2 \leq E \leq 2.1$ MeV: type (v) is higher by 3% at 0.7 MeV and lower by 4.2% at 2.1 MeV than the Brice form. All other forms deviate from Eq. (6) by less than this amount.

TABLE I. Stopping cross section of carbon (graphite) for α particles. The numbers in parentheses give the estimated probable error in ϵ (expressed as a percent) assigned according to the discussion in Sec. IV.

Brice parameters $(n, a, z) = (3.10, 0.501, 1.02)$ [See Eq. (6)]		
Energy (MeV)	$dE/\rho dx$ (keV cm^2/μg)	ϵ (10^{-15} eV cm^2)
0.3	1.94	38.7 (3.5%)
0.4	2.05	40.7 (3.5%)
0.5	2.08	41.5 (3.5%)
0.6	2.06	41.2 (3.5%)
0.7	2.03	40.5 (3.5%)
0.8	1.98	39.5 (3.5%)
0.9	1.93	38.5 (3.5%)
1.0	1.87	37.4 (3.5%)
1.1	1.82	36.3 (3.5%)
1.2	1.77	35.3 (3.5%)
1.3	1.72	34.3 (3.6%)
1.4	1.67	33.3 (3.7%)
1.5	1.62	32.4 (3.9%)
1.6	1.58	31.6 (4.0%)
1.7	1.54	30.8 (4.2%)
1.8	1.50	30.0 (4.4%)
1.9	1.47	29.3 (4.6%)
2.0	1.44	28.7 (4.8%)

As a general check of the experimental technique, some data were also collected at $\theta_L = 130.0°$. The values of $\epsilon(E)$ obtained at this alternative scattering angle agreed with those obtained at θ_L to within the assigned uncertainty.

IV. ACCURACY

The experimental uncertainities in the effective stopping cross section $\epsilon_{\text{eff}}(E_{10})$ arise from errors in the various quantities that appear in Eq. (1). Hill[29] has shown that the elastic scattering cross section $^{12}C(\alpha,\alpha)^{12}C$ has no anomalies below 2.5 MeV. The shell-shielded Coulomb potential is known to be quite accurate[30] below the Coulomb barrier for heavier elements, and the screening corrections are essentially negligible for $^{12}C(\alpha,\alpha)^{12}C$ except at the lowest bombarding energies. The terminal voltage of the Van de Graaff accelerator was measured with a generating voltmeter calibrated to ±0.15% using standard nuclear-reaction calibration energies.[31] The laboratory scattering angle θ_L and angle of incidence θ_1 were known to within ±0.1°. These various sources of error combine to an error of <1% in $\epsilon_{\text{eff}}(E_{10})$.

The primary sources of error in ϵ_{eff} were (i) the uncertainty in $N_0\Delta\Omega$, estimated to be ±3%; (ii) the error in the yield $y(E_{10}, \alpha E_{10})$ at the midpoint of the step in Fig. 1, estimated to be ±2%; and (iii) the error in the width of the energy interval in the spectrum, estimated to be ±1%. Thus, the total probable error in $\epsilon_{\text{eff}}(E_{10})$ is estimated to be <4% when all errors are added in quadrature.

The probable error in the stopping cross section $\epsilon(E_{\text{int}})$ calculated by the first data-reduction scheme is estimated to be $\gtrsim$4% for $0.3 \leq E_{\text{int}} \leq 1.575$ MeV. The probable error in $\epsilon(E)$ by the second data-reduction scheme is found by first determining the error in the Brice-function parameters (n, a, z) of Eq. (6) from the error matrix of the least-squares fit[32] and then by expanding the error in $\epsilon(E)$ in terms of the errors in these parameters.[33] This probable error in $\epsilon(E)$ for the Brice function is found to be small (<1% at 0.3 MeV to 2.4% at 2.0 MeV); however, the various fitting functions (see Sec. III) differ from the Brice form from 3% at 0.7 MeV to 4.2% at 2.1 MeV. We have therefore assigned a probable error to the $\epsilon(E)$ values in Table I which is essentially a compromise between the errors of the two data-reduction methods, and which allows for error due to different fitting functions. The increase in error at the higher energies is caused by the scattering geometry used in the experiment. For $\theta_L = 90.0°$, $\theta_1 = \theta_2 = 45.0°$, $\alpha = 0.5001$, $\beta = 1.000$, so that E_{10} and αE_{10} are widely separated for large E_{10}. Thus, $\epsilon_{\text{eff}}(E_{10}) = 0.5\epsilon(E_{10}) + 1.00\epsilon(\alpha E_{10})$ is essentially a weighted average of $\epsilon(E_{10})$ and (αE_{10}), with twice the weight being given to $\epsilon(\alpha E_{10})$.

V. RESULTS

The measured effective stopping cross sections $\epsilon_{\text{eff}}(E_{10})$ of graphite and vapor-deposited carbon are shown in Fig. 2 as the closed circles and crosses, respectively. The solid and dashed curves are the Brice curve fit [Eq. (6)] according to the second data-reduction scheme using n,a,z $(n',a',z') = 3.10,\ 0.501,\ 1.02$ (3.40, 0.392, 1.37) for 41 (26) spectra for graphite (vapor-deposited

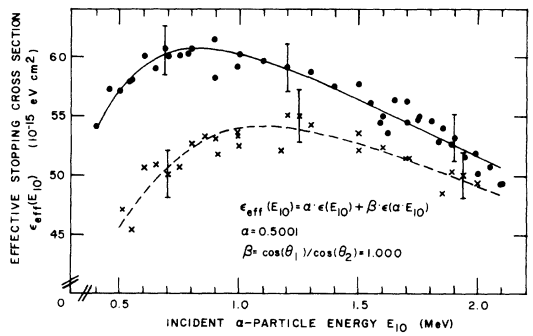

FIG. 2. Effective stopping cross section $\epsilon_{\text{eff}}(E_{10}) = \alpha\,\epsilon(E_{10}) + \beta\,\epsilon(\alpha E_{10})$ as a function of incident α-particle energy E_{10}. The closed circles and crosses are the experimental values for graphite and amorphous thin films, respectively. The solid and dashed curves represent the Brice curve fit [Eq. (6)] according to the second data-reduction scheme using n,a,z, $(n',a',z') = 3.10,\ 0.501,\ 1.02$ (3.40, 0.392, 1.37) for graphite (vapor-deposited amorphous carbon).

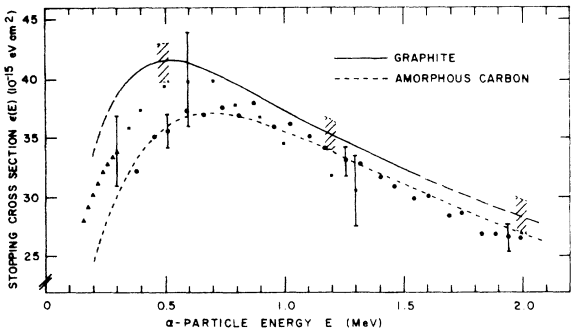

FIG. 3. Stopping cross section $\epsilon(E)$ of carbon α particles. The upper curve is for graphite, and the lower curve is for amorphous vapor-deposited carbon. The solid portion of the upper curve is for the energy region in which the iteration procedure (see text) and the Brice curve fit apply and give identical values of $\epsilon(E)$. The dashed portion of the upper curve is the Brice curve fit [Eq. (6)] with $n,a,z = 3.10,\ 0.501,\ 1.02$. The dotted curve is the Brice fit for amorphous carbon with $n',a',z' = 3.40,\ 0.392,\ 1.37$. The cross hatching on the upper curve is the estimated probable error in $\epsilon(E)$ as given in Table I. The thin-target measurements of ϵ by Chu and Powers (Ref. 9), Sautter and Zimmerman (Ref. 8), and by Porat and Ramavataram (Ref. 7) are given, respectively, by closed circles, triangles, and squares. The figure gives clear evidence of the allotropic effect in carbon indicated in the text.

amorphous carbon). In Fig. 3 the stopping cross sections ϵ(C) for graphite and amorphous vapor-deposited carbon are shown as the upper and lower curves, respectively. The solid portion of the upper curve is for the energy region in which the iteration procedure and the Brice curve fit apply and give identical values of $\epsilon(E)$. The dashed portion of the upper curve is the Brice curve fit with $n,a,z = 3.10,\ 0.501,\ 1.02$. These values of $\epsilon(E)$ are entered in Table I along with their estimated probable error expressed as a percent according to the discussion of Sec. IV. The dotted curve in Fig. 3 is the Brice curve fit for amorphous carbon with $n',a',z' = 3.40,\ 0.392,\ 1.37$. The agreement between the thin-film vapor-deposited carbon $\epsilon(E)$ of Chu and Powers[9] (probable error ±4.2%) and thin-film vapor-deposited $\epsilon(E)$ presented here (dotted curve), but calculated by the thick-target method, is quite good. The stopping cross section $\epsilon(E)$ of graphite, however, is significantly higher than either previously reported values, or the present measurements, for vapor-deposited thin-carbon films.

The discrepancy between graphite $\epsilon(E)$ and the thin-film vapor-deposited $\epsilon(E)$ is greatest ($\simeq 20\%$) in the energy region of maximum $\epsilon(E)$, the region in which electrons in the valence states of C account for the bulk of the energy loss. The graphite $\epsilon(E)$ is still higher than vapor-deposited $\epsilon(E)$ by $\simeq 6\%$ for $E > 1.5$ MeV. As explained in Sec. IV, however, the probable error in this region ($\simeq 5\%$) is also larger than that ($\simeq 3.5\%$) at lower energies. Since the error increases with increasing energy, the curve should not be extrapolated outside the energy region for which it was measured. This increase in error with increasing energy does not obviate the conclusion that the stopping cross sections of these two allotropes of carbon differ markedly below 1.0 MeV.

Although a comprehensive theory of stopping cross sections is not available for the energy region $0.3 \leq E_\alpha \leq 2.0$ MeV, the findings of this experiment are not inconsistent with the results of electron energy-loss measurements in the different allotropes of carbon. Three types of electron excitation are possible in carbon[34]: (i) single-electron transitions from the K shell to the valence and conduction bands; (ii) transitions (intraband and interband) of valence electrons; and (iii) collective or plasma oscillations[35] of the valence electrons.[36] The stopping cross section is ofter characterized[37] by the mean excitation potential I. For K-shell excitation, Walske[28] has shown that as I_K increases, the stopping cross section decreases. Egerton *et al.*[38] have obtained from energy-loss spectra the energy (> 280 eV) and density of final states for excitation of K-shell electrons to the valence and conduction bands in diamond, graphite, and vapor-deposited carbon. The K-to-π transition revealed a lower density of final states in vapor-deposited carbon than in graphite. The excitation potential is therefore slightly higher for vapor-deposited carbon than for graphite, and the stopping cross section would therefore be slightly higher for graphite than for vapor-deposited carbon. The predicted contribution from K-shell excitation to the stopping cross section is in agreement with that seen in the present experiment.

Interband transitions of valence electrons account for electron energy losses[36] of 50–280 eV. An overlap of valence and conduction bands is indicated[39] for graphite, but a larger band gap occurs in diamond.[40] Although the structure of vapor-deposited thin-film carbon is not well established, the structural model of Kakinoki *et al.*[11] would indicate a band structure, and therefore, an excitation potential higher for vapor-deposited carbon than graphite but lower than diamond. Thus, the stopping cross section (based on the Bethe-Bloch approach[37]) for vapor-deposited carbon would be less than that for graphite since the contribution to I from the interband transitions is greater for the former than for the latter.

The above two effects (K-shell excitation and

interband transitions) are consistent with a distinct chemical or allotropic effect in the stopping cross section of carbon. The contribution from the collective or plasmon excitations to the stopping cross section for C does not explicitly indicate whether the difference between graphite and vapor-deposited stopping cross sections is due to a density effect (as proposed by Ziegler and Brodsky[41] for Si, which is similar in chemical structure to C) or to an allotropic or chemical effect. The energies of this $\pi+\sigma$ ($\simeq 25$ eV) and π ($\simeq 7$ eV) excitations depend on the mean density of electrons,[21] n, and the excitations observed in diamond[42] have a higher plasma frequency ω_p than observed in graphite, while the relative strength of the lower π excitation is less in vapor-deposited carbon than in graphite.

Finally, it might be mentioned that Brandt[43] predicted the mean excitation potential for graphite to be 12% lower than carbon appearing in aliphatic hydrocarbons. Single-bonded aliphatic hydrocarbons have been shown to give a carbon stopping cross section (calculated from Bragg's additivity rule) that is in excellent agreement with the values of vapor-deposited carbon.[5]

Thus, it is seen that the results of this experiment are in qualitative agreement with the results of electron-energy-loss spectra and with hydrocarbon stopping-cross-section measurements. The present results suggest that an allotropic effect does indeed exist.

ACKNOWLEDGMENTS

One of the authors (S.M.) wishes to express his gratitude to Professor Thomas C. Franklin of the Baylor University Chemistry Department for many stimulating discussions on the structure and composition of various forms of carbon, and to Ron Robbins for making electron-diffraction patterns of the thin carbon films. The authors also wish to thank Professor K. H. Wang of the Baylor University Physics Department for his many helpful comments. Grateful appreciation is also given to the Baylor University Research Committee for funds to pay for the publication costs of this paper.

---

*Research supported in part by the Robert A. Welch Foundation, Houston, Texas 77002.

[1]P. D. Bourland, W. K. Chu, and D. Powers, Phys. Rev. B 3, 3625 (1971).
[2]P. D. Bourland and D. Powers, Phys. Rev. B 3, 3635 (1971).
[3]D. Powers, W. K. Chu, R. J. Robinson, and A. S. Lodhi, Phys. Rev. A 6, 1425 (1972).
[4]D. Powers, A. S. Lodhi, W. K. Lin, and H. L. Cox, Jr., Thin Solid Films 19, 205 (1973).
[5]A. S. Lodhi and D. Powers, Phys. Rev. A 10, 2131 (1974).
[6]G. W. Gobeli, Phys. Rev. 103, 275 (1956).
[7]D. I. Porat and K. Ramavataram, Proc. Phys. Soc. Lond. 78, 1135 (1961).
[8]C. A. Sautter and E. J. Zimmerman, Phys. Rev. 140, A490 (1965).
[9]W. K. Chu and D. Powers, Phys. Rev. 187, 478 (1969).
[10]R. D. Heidenreich, J. Electromicrosc. (Tokyo) 16, 23 (1967).
[11]J. Kakinoki, K. Katada, J. Hanawa, and T. Ino, Acta Crystallogr. 13, 171 (1960).
[12]S. D. Softky, Phys. Rev. 123, 1685 (1961).
[13]L. C. Northcliffe and R. F. Schilling, Nucl. Data Tables A 7, 233 (1970).
[14]*Handbook of Thin Film Technology*, edited by L. I. Maissel and R. Glang (McGraw-Hill, New York, 1970), pp. 1–40.
[15]D. E. Bradley, Brit. J. Appl. Phys. 15, 65 (1954).
[16]R. Schaeffer and R. K. Pearson, J. Am. Chem. Soc. 91, 2153 (1969).
[17]S. H. Mahan, *University Chemistry* (Addison-Wesley, Reading, Mass., 1965) p. 492.
[18]W. A. Wenzel and W. Whaling, Phys. Rev. 87, 499 (1952).
[19]Forest S. Mozer, Ph.D. thesis (California Institute of Technology, 1956) (unpublished).
[20]*Index (Inorganic) Power Diffraction File*, ASTM Pub. No. PDIS16i, edited by J. V. Smith (American Society for Testing and Materials, Philadelphia, 1966).
[21]L. B. Leder and J. A. Suddeth, J. Appl. Phys. 31, 1422 (1960).
[22]Wayne E. Bailey, M. S. thesis (Baylor University, Waco, Tex., 1969) (unpublished).
[23]W. K. Lin, S. Matteson, and D. Powers, Phys. Rev. B 10, 3746 (1974).
[24]C. W. Snyder, S. Rubin, W. A. Fowler, and C. C. Lauritsen, Rev. Sci. Instrum. 21, 852 (1950).
[25]F. T. Smith, R. P. Marchi, W. Aberth, D. C. Lorents, and O. Heinz, Phys. Rev. 161, 31 (1967).
[26]B. M. Shchigolev, in *Mathematical Analysis of Observations* (American Elsevier, New York, 1965), pp. 243–247.
[27]D. K. Brice, Phys. Rev. A 6, 1791 (1972).
[28]M. C. Walske, Phys. Rev. 88, 1283 (1952); 101, 940 (1956).
[29]R. W. Hill, Phys. Rev. 90, 845 (1953).
[30]A. v. Wijngaarden, E. J. Brimmer, and W. E. Baylis, Can. J. Phys. 48, 1835 (1970).
[31]J. B. Marion, Rev. Mod. Phys. 38, 660 (1966).
[32]J. Mathews and R. L. Walker, *Mathematical Methods of Physics* (Benjamin, New York, 1964), p. 367.
[33]C. G. Paradine and B. H. P. Rivett, *Statistics for Technologists* (Van Nostrand, New York, 1953), p. 103.
[34]Y. H. Ichikawa, Phys. Rev. 109, 653 (1958).
[35]D. Pines, Rev. Mod. Phys. 28, 184 (1956).
[36]R. F. Egerton, Philos. Mag. 31, 199 (1975).
[37]H. A. Bethe and J. Ashkin, in *Experimental Nuclear Physics*, edited by E. Segre (Wiley, New York, 1953), Vol. I, p. 166.

[38]R. F. Egerton and M. J. Whelan, J. Electron Spectrosc. Relat. Phenom. 3, 232 (1974).
[39]R. F. Willis, B. Fitton, and G. S. Painter, Phys. Rev. B 9, 1926 (1974).
[40]G. S. Painter, D. E. Ellis, and A. R. Lubinsky, Phys. Rev. B 4, 3610 (1971).
[41]J. F. Ziegler and M. H. Brodsky, J. Appl. Phys. 44, 188 (1973).
[42]N. R. Whetten, Appl. Phys. Lett. 8, 135 (1966).
[43]W. Brandt, Phys. Rev. 104, 691 (1956).